ISSN 0036-0236, Russian Journal of Inorganic Chemistry, 2016, Vol. 61, No. 2, pp. 239–242. © Pleiades Publishing, Ltd., 2016.
Original Russian Text © P.P. Fedorov, V.K. Goncharuk, I.G. Maslennikova, I.A. Telin, T.Yu. Glazunova, 2016, published in Zhurnal Neorganicheskoi Khimii, 2016, Vol. 61, No. 2, pp. 252–255.

PHYSICOCHEMICAL ANALYSIS OF INORGANIC SYSTEMS

Diagram of the PbF_2–SnF_2 System

P. P. Fedorov[a], V. K. Goncharuk[b], I. G. Maslennikova[b], I. A. Telin[b], and T. Yu. Glazunova[c]

[a] *Prokhorov General Physics Institute, Russian Academy of Sciences, ul. Vavilova 38, Moscow, 119991 Russia*
[b] *Institute of Chemistry, Far-East Branch, Russian Academy of Sciences, pr. Stoletiya Vladivostoka 159, Vladivostok, Russia*
[c] *Moscow State University, Moscow, 119991 Russia*
e-mail: ppf@lst.gpi.ru

Received May 30, 2015

Abstract—A phase diagram of the PbF_2–SnF_2 system has been studied by differential thermal analysis and X-ray powder diffraction. The system forms $Pb_{1-x}Sn_xF_2$ ($x \leqslant 0.33$) solid solution and three compounds. Pb_2SnF_6 decomposes in solid state by a peritectoid reaction at 350°C; $Pb_3Sn_2F_{10}$ and $PbSnF_4$ melt by peritectic reactions at 565 and 380°C, respectively. The eutectic coordinates are 180°C, 90 mol % SnF_2.

DOI: 10.1134/S0036023616020078

The compound $PbSnF_4$ has a maximal anionic conductivity among the fluoride-ion conductors [1]. These properties of $PbSnF_4$ were discovered at the Laboratory of Solid State Chemistry (Bordeaux, France), headed by Hagenmuller [2–4]. Abundant documentation concerns electrochemical properties, polymorphism, and preparation of $PbSnF_4$ (see, e.g., [3–14]). Many lead fluoride-based [1, 15–18] and tin-based [1, 19, 20] compounds and solid solutions have been studied for finding fluoride-conductive solid electrolytes and for recognizing the trends of high anionic conductivity.

Phase equilibria in the PbF_2–SnF_2 system have been studied incompletely. Some data were obtained in the synthesis and characterization of solid electrolytes. $PbSnF_4$ is a compound having complex polymorphism [3, 5] (Fig. 1). All of its polymorphs have fluorite-like structures. The lattice symmetry increases, as temperature rises, from orthorhombic (monoclinic) (α) through tetragonal (β) to cubic (γ).

Studies of the title system in solid state showed the formation of fluorite solid solutions $Pb_{1-x}Sn_xF_2$, where $x \leqslant 0.3$, with the saturation boundary being $x = 0.25$ at 350°C [6]. Two fluorite-like phases were found to exist, β''' and β'', whose compositions approximately correspond to compounds Pb_2SnF_6 and Pb_3SnF_{10}, respectively. These phases have tetragonally distorted fluorite lattice, just as β-$PbSnF_4$, but with differing superstructures.

Tin(II) fluoride compounds have unusual crystal chemistry due to the stereochemically active lone pair of Sn^{2+} [21]. This specific feature facilitates the formation of SnF_2-containing fluoride glasses [22–25].

Our goal in this study was to construct a PbF_2–SnF_2 phase diagram and elucidate the melting characters of phases and the specifics of their equilibration with melt. Preliminary data pertaining to the 50–100% SnF_2 region can be found in the survey [26]. Here we continue our studies into phase diagrams in PbF_2–MF_2, where M = Mg [27], Ca, Sr [28], Ba [29], and Cd [30] systems.

EXPERIMENTAL

We tested two protocols. In the region where compositions are rich in lead fluoride, we used the protocol similar to that we used earlier to study the PbF_2–ZrF_4 phase diagram [31]. A lead difluoride sample (high purity grade) was vacuum dried at 300–350°C for 1 h. Tin difluoride was prepared by fluoriding metallic tin (a pure for analysis grade sample) with ammonium hydrodifluoride [32]. After the ammonium fluoride was removed almost completely, the thus-prepared SnF_2 containing minor $NH_4Sn_2F_5$ was recrystallized from hydrofluoric acid over metallic tin.

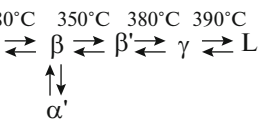

Fig. 1. Scheme of polymorphic transformations in $PbSnF_4$ according to Perez et al. [5].

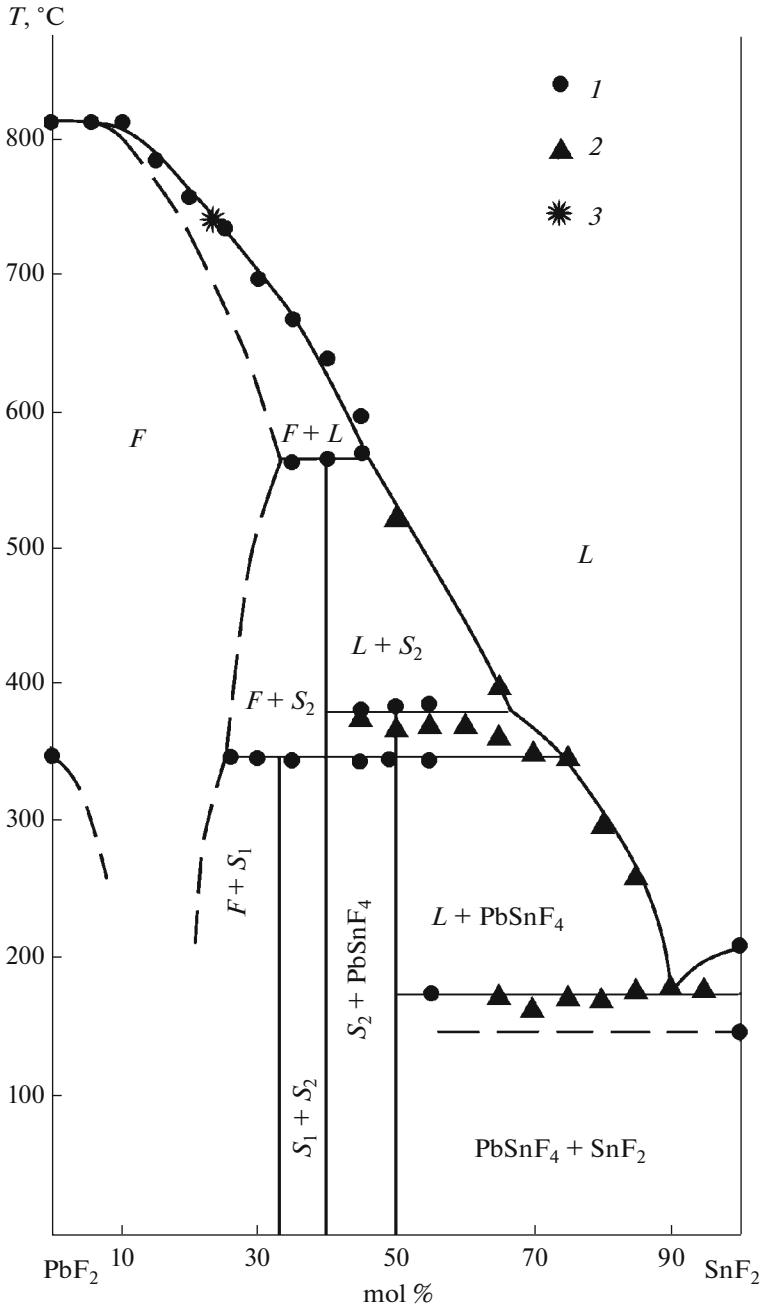

Fig. 2. PbF_2–SnF_2 phase diagram. Notations: L = melt, $F = Pb_{1-x}Sn_xF_2$ fluorite solid solution, $S_1 = Pb_2SnF_6$, $S_2 = Pb_3Sn_2F_{10}$. (*1*) platinum crucibles, (*2*) graphite crucibles, and (*3*) borrowed from [2, 4].

The resulting tin difluoride was dried for 24 h in air, then pounded in a mortar for 5 min, and vacuum dried at 100°C. A sample with a total weight of 5 g was stirred at room temperature in a Pulverisette 7 premium line (FRITSCH) planetary micromill at 800 rpm for 60 min (six 10-min cycles). Reverse was up; the working body was made of zirconia. Samples to be milled were charged in and discharged from milling beakers inside a drybox. Milled samples were stored inside a drybox filled with argon and cells with P_2O_5. Differential thermal analysis (DTA) was performed on an MOM Q-1000 instrument interfaced with a computer. Samples were transferred to DTA crucibles inside a drybox. A crucible was mounted in a special designed construct for heating a sample in a covered crucible under the vapor pressure of the sample with an access of air being precluded to the maximal possible degree. Platinum crucibles were used; the heating rate was 5 K/min. The measurement accuracy was ±5 K/min; sample sizes were 0.90–0.95 g.

In the tin fluoride-rich region, the protocol was similar to the one we used to study PbF_2–MF_2 phase diagrams. The initial reagents used were PbF_2 (high purity grade) remelted under the fluorinating atmosphere of Teflon pyrolysis products. Tin difluoride was prepared as described elsewhere [32] and also remelted under a fluorinating atmosphere.

Used were an air-tight degassible setup to be filled with helium, graphite crucibles, and W 5% Re–W 20% Re thermocouples; samples sizes were 1.5–2 g. The heating and cooling rates were 10 K/min. Vaporization loss was negligible, but we noticed a very strong adherence of SnF_2 melt to graphite, so the melt escaped from the crucible.

In interpreting thermoanalytical curves, we determined liquidus temperatures as the onset temperatures of cooling curve peaks. Earlier we showed that lead fluoride and its base solid solution in melts are not prone to undercooling [33]. In interpreting heating curves the temperatures corresponding to invariant transformations were taken to be the onset temperatures of endotherms. The temperatures of monovariant transformations (on liquidus curves) were determined as the peak temperatures of the peaks minus a correction [34], which equaled 10°C for platinum crucibles and 20°C for graphite crucibles.

RESULTS AND DISCUSSION

Figure 2 shows the resulting PbF_2–SnF_2 phase diagram. The system forms $Pb_{1-x}Sn_xF_2$ ($x \leqslant 0.33$) solid solutions and three compounds. Pb_2SnF_6 decomposes in solid state by a peritectoid reaction at 350°C. $Pb_3Sn_2F_{10}$ and $PbSnF_4$ melt by peritectic reactions at 565 and 380°C, respectively. The eutectic coordinates are 180°C, 90 mol % SnF_2. Different DTA protocols gave similar results. The melting point of a $Pb_{0.7}Sn_{0.3}F_2$ sample determined in [2, 4] corresponds with our liquidus curve.

The $PbSnF_4$, melting point is reported to be 390°C, which well agrees with our measurements. However, from our phase diagram it flows that $PbSnF_4$ melting is incongruent and follows the reaction

$$PbSnF_4 \leftrightarrow Pb_3Sn_2F_{10} + L,$$

where the melt L contains 67 mol % SnF_2. The complete melting of the sample of this composition occurs at 570°C.

The boundary of the $Pb_{1-x}Sn_xF_2$ solid solution field is temperature dependent and, on the whole, corresponds with literature data. The highest solubility at 565°C is $x \leqslant 0.33$. Solid solution ordering is not continuous as suggested by, for example, Vilminot et al. [6], but rather is discontinuous. The existence of homogeneity regions of ordered phases (compounds $PbSnF_4$, Pb_2SnF_6, and $Pb_3Sn_2F_{10}$) needs to be studied separately. The high-temperature cubic γ phase of $PbSnF_4$ may be treated as a berthollide formed due to cutting the $Pb_{1-x}Sn_xF_2$ fluorite solid solution field by a set of ordered phases [35, 36].

Near the lead fluoride point, the solidus and liquidus curves almost merge and have (to the accuracy of experiment) a horizontal tangent. This means that the tin distribution coefficient upon crystallization is near unity and corresponds to the formation of a tangential extreme [37]. The situation favors the preparation of homogeneous crystals when lead difluoride is doped with tin.

The melting curves that feature three congruent melting peaks in the range 40–100% SnF_2 as reported by Donaldson and Senior [38], are likely to be artifacts.

REFERENCES

1. A. K. Ivanov-Shits and I. V. Murin, *Solid-State Ionics* (Izd–vo SPbGU, St. Petersburg, 2010), Vol. 2 [in Russian].
2. A. Rhandor, These de la Docteur en chimie et physique des materaux (L'Universite de Bordeaux I, 44, 1979).
3. J. M. Reau, C. Lucat, J. Portier, and P. Hagenmuller, Mater. Res. Bull. **13**, 877 (1978).
4. C. Lucat, A. Rhandor, L. Cot, and J. M. Reau, Solid State Commun. **32**, 167 (1979).
5. G. Perez, S. Vilminot, and W. Granier, Mater. Res. Bull. **15**, 587 (1980).
6. S. Vilminot, G. Perez, W. Granier, and L. Cot, Solid State Ionics **2**, 91 (1981).
7. P. Lagassie, J. Grannec, and J. M. Reau, Solid State Ionics **21**, 343 (1986).
8. S. V. Chernov, A. L. Moskvin, and I. V. Murin, Solid State Ionics **47**, 71 (1991).
9. Y. Ito, T. Mukoyama, H. Funatomi, et al., Solid State Ionics **67**, 301 (1994).
10. R. Kanno, K. Ohno, H. Izumi, et al., Solid State Ionics 70–71, 253 (1994).
11. A. Collin and G. Denes, D. Le Roux, et al., Intern. J. Inorg. Mater. **1**, 289 (1999).
12. N. I. Sorokin and P. P. Fedorov, O. K. Nikol'skaya, et al., Inorg. Mater. **37**, 1178 (2001).
13. S. Yoshikado, Y. Ito, and J. M. Reau, Solid State Ionics **154–155**, 503 (2002).
14. M. Uno, M. Onitsuka, Y. Ito, and S. Yoshikado, Solid State Ionics **176**, 2493 (2005).
15. J. M. Reau, N. Elomari, J. Senegas, and P. Hagenmuller, Mater. Res. Bull. **24**, 1441 (1989).
16. N. I. Sorokin and P. P. Fedorov, Inorg. Mater. **33**, 1 (1997).
17. V. Ya. Kavun, A. B. Slobodyuk, E. A. Tararako, et al., Inorg. Mater. **43**, 301 (2007).
18. V. Trnovcova, P. P. Fedorov, I. I. Buchinskaya, et al., Solid State Ionics **119**, 181 (1999).
19. I. V. Murin and S. V. Chernov, Vestn. Leningr. Univ., No. 10, 105 (1982).
20. G. Denes, T. Birchall, M. Sayer, and M. F. Bell, Solid State Ionics **13**, 213 (1984).

21. Yu. V. Kokunov and I. E. Rakov, Zh. Neorg. Khim. **40**, 583 (1995).
22. E. B. Merculov, V. K. Goncharuk, and S. A. Stepanov, J. Non-Cryst. Solids **170**, 65 (1994).
23. P. J. Newman and H. Downes, J. Non-Cryst. Solids **213–214**, 116 (1997).
24. P. P. Fedorov, Crystallogr. Repts **42**, 1064 (1997).
25. P. P. Fedorov, Inorg. Mater. **33**, 1197 (1997).
26. I. I. Buchinskaya and P. P. Fedorov, Russ. Chem. Rev **73**, 371 (2004).
27. P. P. Fedorov, I. I. Buchinskaya, O. S. Bondareva, et al., Zh. Neorg. Khim. **40**, 1380 (1995).
28. I. I. Buchinskaya and P. P. Fedorov, Russ. J. Inorg. Chem. **43**, 1106 (1998).
29. I. I. Buchinskaya, O. L. Evdokimova, P. P. Fedorov, and B. P. Sobolev, Crystallography Reports **39**, 480 (1994).
30. V. Trnovcova, P. P. Fedorov, M. Ozvoldova, et al., J. Optoelectron. Adv. Mater. **5**, 627 (2003).
31. E. B. Merculov, G. D. Lukiyanchuk, V. K. Goncharuk, et al., Proc. ISIF-2006. The Second International Siberian Worksop INTERSIBFLUORINE-2006 “Advanced Inorganic Fluorides”. Tomsk, 11–16 June 2006. P. 169.
32. E. G. Rakov and T. V. Goryacheva, Russ. J. Inorg. Chem. **45**, 1006 (2000).
33. I. I. Buchinskaya and P. P. Fedorov, Europhys. Lett. **83**, 16001 p1-p2 (2008).
34. P. P. Fedorov and L. V. Medvedeva, Russ. J. Inorg. Chem. **34**, 1528 (1989).
35. P. P. Fedorov, P. I. Fedorov, and B. P. Sobolev, Zh. Neorg. Khim. **18**, 3319 (1973).
36. P. P. Fedorov, Russ. J. Inorg. Chem. **57**, 959 (2012).
37. P. P. Fedorov, Zh. Neorg. Khim. **31**, 759 (1986).
38. J. D. Donaldson and B. J. Senior, J. Chem. Soc. A, 1821 (1967).

Translated by O. Fedorova